

Search for D^0 meson decays to $\pi^+\pi^-e^+e^-$ and $K^+K^-e^+e^-$ final states

R. Aaij *et al.**
(LHCb Collaboration)

 (Received 17 December 2024; accepted 18 March 2025; published 5 May 2025)

A search for D^0 meson decays to the $\pi^+\pi^-e^+e^-$ and $K^+K^-e^+e^-$ final states is reported using a sample of proton-proton collisions collected by the LHCb experiment at a center-of-mass energy of 13 TeV, corresponding to an integrated luminosity of 6 fb^{-1} . The decay $D^0 \rightarrow \pi^+\pi^-e^+e^-$ is observed for the first time when requiring that the two electrons are consistent with coming from the decay of a ϕ or ρ^0/ω meson. The corresponding branching fractions are measured relative to the $D^0 \rightarrow K^-\pi^-[e^+e^-]_{\rho^0/\omega}$ decay, where the two electrons are consistent with coming from the decay of a ρ^0 or ω meson. No evidence is found for the $D^0 \rightarrow K^+K^-e^+e^-$ decay and world-best limits are set on its branching fraction. The results are compared to, and found to be consistent with, the branching fractions of the $D^0 \rightarrow \pi^+\pi^-\mu^+\mu^-$ and $D^0 \rightarrow K^+K^-\mu^+\mu^-$ decays recently measured by LHCb and confirm lepton universality at the current precision.

DOI: [10.1103/PhysRevD.111.L091101](https://doi.org/10.1103/PhysRevD.111.L091101)

Within the standard model (SM), flavor-changing neutral-current (FCNC) processes are suppressed by the Glashow-Iliopoulos-Maiani mechanism [1]. Extensions of the SM can, however, significantly alter the probabilities at which these processes occur. Depending on the nature of potential beyond-SM (BSM) contributions, measurements of observables sensitive to FCNCs can probe energy scales of tens or even hundreds of TeV [2], providing a powerful tool in characterizing the allowed parameter space of BSM physics.

Rare charm decays may proceed via FCNC $c \rightarrow u\ell^+\ell^-$ transitions ($\ell = \mu$ or e). In the SM, these so-called *short-distance* contributions result in branching fractions of $\mathcal{O}(10^{-9})$ [3] for decays of the type $D \rightarrow X\ell^+\ell^-$, where X is one or more hadrons. The experimentally observable $D \rightarrow X\ell^+\ell^-$ decays are, however, dominated by *long-distance* processes involving intermediate hadronic resonances such as $D \rightarrow XY(\rightarrow \ell^+\ell^-)$ where Y is a hadronic resonance, *e.g.* a ρ^0 , ω or ϕ meson. These resonances enhance the SM branching fractions but remain suppressed at the level of $\mathcal{O}(10^{-6})$ [3–6], with the broadest resonances spanning the entire dilepton-mass spectrum. Accessing the short-distance contributions of interest therefore requires both large datasets and the use of complementary observables that are sensitive to short- and long-distance

processes, such as angular distributions, charge-parity asymmetries or tests of lepton universality [5–19].

Due to the universality of the electroweak interaction couplings to leptons in the SM, any differences in meson decay rates into final states with leptons of different generations arise purely from lepton mass effects. Consequently, comparing the branching fraction of a decay mode with muons in the final state to its counterpart with electrons provides a powerful probe of BSM effects, despite the dominance of long-distance contributions and large uncertainties in the SM prediction for the individual decay modes. Depending on the properties of possible BSM contributions in $c \rightarrow u\ell^+\ell^-$ transitions, the validity of lepton universality could be broken at the percent level [6].

The $D^0 \rightarrow h^+h^-\mu^+\mu^-$ decays ($h = \pi$ or K) were first observed by the LHCb Collaboration [20], which subsequently studied their angular structure and charge-parity asymmetries [21,22]. Charge-conjugate decays are implied throughout the paper. The $D^0 \rightarrow h^+h^-e^+e^-$ decays offer the opportunity to probe the validity of lepton universality. However, electron final states are more challenging experimentally, in particular because the electrons lose a significant fraction of their energy as bremsstrahlung radiation while passing through the detector material. Until now, only upper limits on the branching fractions of $D^0 \rightarrow h^+h^-e^+e^-$ decays have been reported [23,24].

This paper reports the first search for the $D^0 \rightarrow \pi^+\pi^-e^+e^-$ and $D^0 \rightarrow K^+K^-e^+e^-$ decays at the LHCb experiment and opens the door for the first lepton universality tests with such decays. The analysis uses pp collision data collected between 2015 and 2018 at a

*Full author list given at the end of the Letter.

center-of-mass energy $\sqrt{s} = 13$ TeV, corresponding to an integrated luminosity of 6 fb^{-1} . The analysis method closely follows that of the LHCb analysis which observed the analogous decays with muons [20]; however the dielectron final state requires the development of a specific selection and reconstruction. The analysis uses D^0 mesons originating from $D^{*+} \rightarrow D^0 \pi^+$ decays with the D^{*+} mesons produced in the primary pp interaction.

The branching fractions of the decays of interest are measured in regions of the dielectron mass relative to the $D^0 \rightarrow K^- \pi^+ [e^+ e^-]_{\rho^0/\omega}$ decay which has a branching fraction of $(4.0 \pm 0.5) \times 10^{-6}$ in the dielectron-mass range $675\text{--}875 \text{ MeV}/c^2$ [25], where the notation indicates that the contribution from the $\rho^0/\omega \rightarrow e^+ e^-$ decay is dominant.

The LHCb detector is a single-arm forward spectrometer covering the pseudorapidity range $2 < \eta < 5$ and is described in detail in Refs. [26,27]. Events are selected by a trigger that consists of a hardware stage, based on information from the calorimeter and muon systems, followed by a software stage which applies a full event reconstruction [28]. The hardware trigger requires the presence of an energy deposit in the electromagnetic calorimeter that may or may not be compatible with originating from the signal candidate, or a muon signature with large transverse momentum which is compatible with originating from any particle in the event. A first stage of the software trigger selects events with either a charged particle that has both a significant transverse momentum and large impact parameter, defined as the minimum distance of the particle trajectory from any primary pp -collision vertex (PV), or with a two-track vertex satisfying a multivariate classifier based on geometric and kinematic criteria which identify the vertex as likely to originate from the decay of a long-lived heavy particle. In a second stage of the software trigger, candidate $D^0 \rightarrow h^+ h^{(\prime)-} e^+ e^-$ decays are selected by combining four tracks that form a secondary vertex separated from any PV. All charged particles are required to have a significant impact parameter, as well as momentum $p > 3 \text{ GeV}/c$ and transverse momentum $p_T > 0.3 \text{ GeV}/c$. The D^0 candidate must have large transverse momentum, a reconstructed mass, $m(D^0)$, in the range $1800\text{--}1950 \text{ MeV}/c^2$ ($1700\text{--}2050 \text{ MeV}/c^2$) for data recorded in the years 2015–2016 (2017–2018) and its momentum vector must be aligned with the vector connecting the PV and the D^0 decay vertex. The larger mass range in the second period is due to a change in the software trigger that allows for improved background studies using information from the sidebands. When more than one PV is reconstructed, the one with respect to which the D^0 candidate has the lowest impact-parameter χ^2 is chosen, defined as the difference in the vertex-fit χ^2 reconstructed with and without the candidate. Finally, $D^{*+} \rightarrow D^0 \pi^+$ candidates are selected by combining the D^0 meson with

a charged particle from the same PV that has $p_T > 120 \text{ MeV}/c$.

Subsequently, signal candidates are further selected off-line by tightening the kinematic and geometric criteria applied in the trigger. A dedicated algorithm associates reconstructed bremsstrahlung photons to tracks identified as electrons; when a given photon is associated with both electron tracks, it is attached to one chosen randomly. Throughout the analysis, signal candidates are split into two periods with different data-taking conditions (2015–2016 and 2017–2018) and further divided into two categories: candidates in which neither electron has an associated bremsstrahlung cluster, and all other candidates, referred to as the no-brem and with-brem categories, respectively. A multivariate classifier is used to remove D^0 candidates containing one or more fake tracks. Stringent particle-identification criteria are then applied to all charged particles to suppress both combinatorial background, from unrelated charged particles, and cross feed backgrounds in which one type of $D^0 \rightarrow h^+ h^{(\prime)-} e^+ e^-$ decay is misidentified as another. The vertex formed by the D^0 and π^+ mesons is constrained to coincide with the PV and the momenta of the particles in the decay chain are updated accordingly. Only candidates with a difference between the reconstructed D^{*+} and D^0 masses, Δm , in the range $144\text{--}147 \text{ MeV}/c^2$ are considered. Further reduction of combinatorial background is achieved using a multivariate selection based on a boosted decision tree (BDT) [29,30]. The following features are used to discriminate signal from background: the momentum, transverse momentum, and impact parameter of the pion from the D^{*+} decay; the fit quality of the D^0 vertex and its separation from the PV; the angle between the D^0 momentum vector and the vector connecting the PV and the D^0 decay vertex; and the fit quality of the D^{*+} vertex. The BDT classifier is trained separately for $D^0 \rightarrow \pi^+ \pi^- e^+ e^-$ and $D^0 \rightarrow K^+ K^- e^+ e^-$ decays, using simulation samples [31,32] as a proxy for the signal and data candidates with $m(D^0)$ greater than $1900 \text{ MeV}/c^2$ as a proxy for the background.

Hadronic $D^0 \rightarrow \pi^+ \pi^- \pi^+ \pi^-$ and $D^0 \rightarrow K^+ K^- \pi^+ \pi^-$ decays, where two pions are misidentified as electrons, constitute a major source of background, which is reduced by a multivariate electron-identification discriminant that combines information from the Cherenkov detectors, the calorimeters and the muon chambers. Finally, selection criteria based on the BDT response and on the electron identification discriminant are optimized by maximizing the figure-of-merit $\epsilon_{h^+ h^- e^+ e^-} / (5/2 + \sqrt{N_{\text{bkg}}})$ [33], where $\epsilon_{h^+ h^- e^+ e^-}$ is the signal efficiency, and N_{bkg} is the total background yield in the $m(D^0)$ range $1700\text{--}1900 \text{ MeV}/c^2$ ($1700\text{--}2050 \text{ MeV}/c^2$) for the no-brem (with-brem) category. The no-brem category has a significantly larger contamination from backgrounds in which hadrons are wrongly identified as electrons and therefore significantly

worse sensitivity to the signals of interest. To facilitate an extrapolation of the yields of misidentified background from the no-brem to the with-brem category, the optimal selection thresholds obtained for the with-brem category are used for the no-brem category. Candidate $D^0 \rightarrow K^- \pi^+ [e^+ e^-]_{\rho^0/\omega}$ decays are selected using the response of the BDT classifier trained on the $D^0 \rightarrow \pi^+ \pi^- e^+ e^-$ ($D^0 \rightarrow K^+ K^- e^+ e^-$) signal when being used to normalize the branching fraction of $D^0 \rightarrow \pi^+ \pi^- e^+ e^-$ ($D^0 \rightarrow K^+ K^- e^+ e^-$). Only one candidate is kept at random if an event contains several signal or normalization candidate decays after the final selection, which happens in less than 0.5% of selected events. To avoid potential biases on the measured signal candidate yields, candidate decays in the $m(D^0)$ signal region were examined only after the analysis procedure was finalized.

Signal and normalization yields are measured with unbinned extended maximum-likelihood fits to the $m(D^0)$ distributions, in regions of the dielectron mass, $m(e^+ e^-)$, which is computed constraining the mass of the

D^0 meson to its known value [34]. The fit results are shown for $D^0 \rightarrow \pi^+ \pi^- e^+ e^-$ and $D^0 \rightarrow K^+ K^- e^+ e^-$ candidates in Figs. 1 and 2, respectively. The fit results for $D^0 \rightarrow K^- \pi^+ [e^+ e^-]_{\rho^0/\omega}$ can be found in the Supplemental Material of this paper [35]. For the signal modes, the $m(e^+ e^-)$ regions are defined in Table I according to the presence of known intermediate resonances and aligned with Ref. [21]. Thus, the lowest $m(e^+ e^-)$ region starts at 2 times the muon mass, m_μ . All fits include four main components: signal, combinatorial background, peaking background from misidentified hadronic decays and background from partially reconstructed D^0 -meson decays, where at least one charged or neutral particle has not been reconstructed. The fit also accounts for the small fraction of $D^0 \rightarrow h^+ h^- e^+ e^-$ decays in which the dielectron pair is produced in one $m(e^+ e^-)$ region and reconstructed in another. All fits are validated to return unbiased results using large numbers of pseudoexperiments. The signal is described with a Crystal Ball [36] distribution for the no-brem category and with a double-sided Crystal Ball distribution for the with-brem category. In both cases, the distribution parameters are determined from simulation. The mass shape of the peaking background is determined using a Bukin distribution [37] fitted to simulated samples of $D^0 \rightarrow h^+ h^{(\prime)-} \pi^+ \pi^-$ decays, where the D^0 mass is calculated by assigning both pion candidates the electron mass. The peaking background in the with-brem category has a small, but not negligible, yield and a shape which is very similar to the signal. Its yield in the with-brem category is extrapolated from the no-brem category using

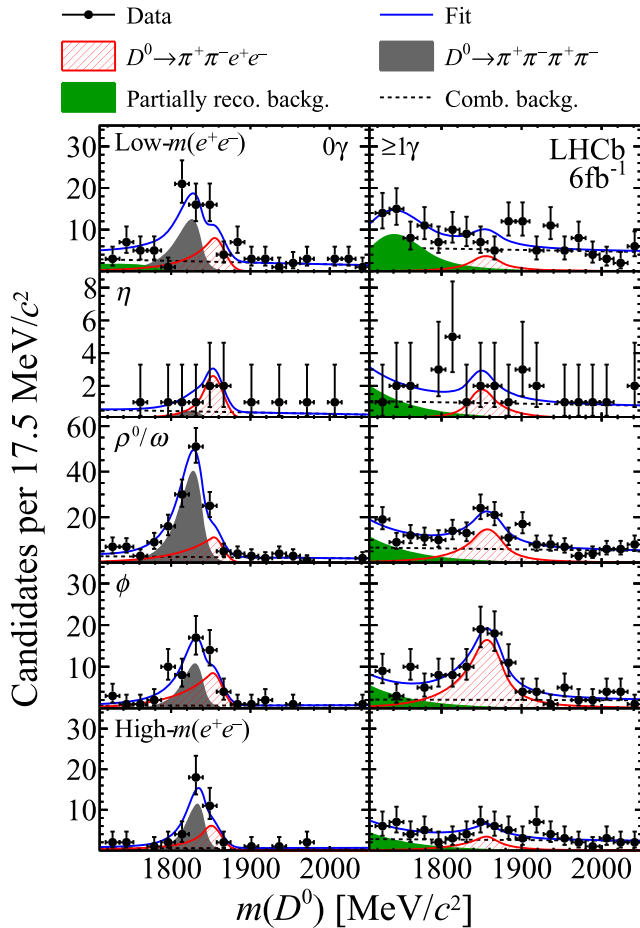


FIG. 1. Mass distributions of selected $D^0 \rightarrow \pi^+ \pi^- e^+ e^-$ candidates in the low- $m(e^+ e^-)$, η , ρ^0/ω , ϕ and high- $m(e^+ e^-)$ regions in the (left, 0γ) no-brem and (right, $\geq 1\gamma$) with-brem categories. Fit projections are also shown.

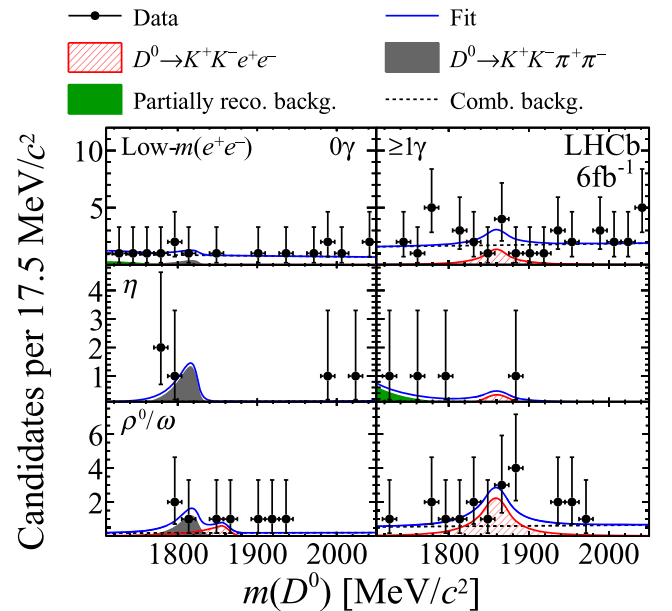


FIG. 2. Mass distributions of selected $D^0 \rightarrow K^+ K^- e^+ e^-$ candidates in the low- $m(e^+ e^-)$, η and ρ^0/ω regions in the (left) no-brem (0γ) and (right) with-brem ($\geq 1\gamma$) categories. Fit projections are also shown.

TABLE I. Yields of (top) $D^0 \rightarrow \pi^+\pi^-e^+e^-$ and (bottom) $D^0 \rightarrow K^+K^-e^+e^-$ signal decays and their significance, \mathcal{S} , in units of Gaussian standard deviations, with respect to zero.

$m(e^+e^-)$ region	[MeV/ c^2]	Yield	\mathcal{S}
$D^0 \rightarrow \pi^+\pi^-e^+e^-$			
Low mass	$2m_\mu$ –525	37 ± 13	2.8σ
η	525–565	10 ± 7	1.6σ
ρ^0/ω	565–950	97 ± 21	5.5σ
ϕ	950–1100	100 ± 18	8.1σ
High mass	> 1100	30 ± 11	2.9σ
$D^0 \rightarrow K^+K^-e^+e^-$			
Low mass	$2m_\mu$ –525	4 ± 8	1.2σ
η	525–565	1 ± 2	1.1σ
ρ^0/ω	> 565	12 ± 7	2.2σ

the relevant efficiencies from simulation. The combinatorial background is described by a first-order polynomial function with its slope determined from data candidates with $\Delta m > 150$ MeV/ c^2 and $m(D^0) > 1900$ MeV/ c^2 . All shape parameters of the signal, peaking background and combinatorial background are fixed. Partially reconstructed backgrounds are modeled using a Bukin distribution fitted to simulated events in the low $m(e^+e^-)$ region (< 525 MeV/ c^2), and an exponential function with its shape parameter determined in the fit to the selected candidates in other $m(e^+e^-)$ ranges. Alternative parametrizations are studied as a source of systematic uncertainty. The yields of each component are allowed to vary in the fits, which are performed simultaneously between the bremsstrahlung categories, periods of data-taking, and dielectron-mass regions. The yield of the combinatorial background is constrained to the yield determined in the Δm sideband 155–165 MeV/ c^2 extrapolated to the signal region.

The resulting signal yields and significances with respect to zero, including statistical and systematic uncertainties, are reported in Table I. Significances exceeding 5 standard deviations are reported for $D^0 \rightarrow \pi^+\pi^-e^+e^-$ decays, where the two electrons are consistent with coming from an intermediate ϕ or ρ^0/ω meson.

The signal yields, $N_{h^+h^-e^+e^-}^i$, in the $m(e^+e^-)$ region i are used to compute the branching fractions as

$$\mathcal{B}^i(D^0 \rightarrow h^+h^-e^+e^-) = \frac{N_{h^+h^-e^+e^-}^i \mathcal{B}(D^0 \rightarrow K^-\pi^+[e^+e^-]_{\rho^0/\omega})}{R_e^i N_{K^-\pi^+e^+e^-}}$$

where $N_{K^-\pi^+e^+e^-}$ is the yield of the normalization mode, which is determined to be 820 ± 39 (875 ± 40) after applying the selection optimized for $D^0 \rightarrow \pi^+\pi^-e^+e^-$ ($D^0 \rightarrow K^+K^-e^+e^-$) decays, while $R_e^i = \epsilon_{h^+h^-e^+e^-}^i / \epsilon_{K^-\pi^+e^+e^-}$ corresponds to the ratio of geometrical acceptances, reconstruction and selection efficiencies of the signal relative to the normalization decays.

The efficiencies are determined using simulated events that are corrected to account for known differences between data and simulation. A particular challenge is the unknown amplitude composition of the decays under study. The signal decays are simulated with an incoherent sum of resonant and nonresonant dimuon and dihadron components. Samples of background-subtracted and efficiency-corrected $D^0 \rightarrow h^+h^{(\prime)-}\mu^+\mu^-$ decays are used to correct the five-dimensional decay model of the corresponding dielectron mode. In addition, particle-identification, hardware-trigger, and tracking efficiencies as well as the dielectron-mass resolution are corrected using dedicated control channels in data.

Systematic uncertainties related to the determination of the yields arise due to limited knowledge of the various fit components and are evaluated using pseudoexperiments, where alternative fit models are tested. These include variations of the signal and background shape parameters within the uncertainties determined from the fits to simulation, and a signal shape obtained with a modified electron momentum resolution. In addition, a Bukin distribution is tested as an alternative distribution to represent the signal. Since not all selection criteria can be applied to background simulation because of limited simulated sample sizes, the misidentified background shapes are recomputed using an alternative set of selection criteria. The combinatorial background shape is determined in alternative Δm ranges. The fraction of signal decays migrating into other regions of dielectron mass is varied within its uncertainty. Furthermore, fit components are reevaluated using simulated samples corresponding to different data-taking years. The dominant systematic uncertainty arising from assumptions in the fit is determined by fully neglecting all partially reconstructed backgrounds. The impact of neglecting further misidentified backgrounds is found to be negligible everywhere except in the signal ρ^0/ω dielectron-mass region, where a contribution from $D^0 \rightarrow K^-\pi^+e^+e^-$ decays misreconstructed as the signal are found, and the appropriate systematic uncertainty is computed. The statistical uncertainty on the normalization yield leads to a relative systematic uncertainty of 4.8% (4.5%) for $D^0 \rightarrow \pi^+\pi^-e^+e^-$ ($D^0 \rightarrow K^+K^-e^+e^-$).

Systematic uncertainties affecting the efficiency ratio include residual data-simulation differences and limitations in the data-driven methods used to determine the particle-identification, tracking and trigger efficiencies. Uncertainties are evaluated directly on the efficiency ratio to take into account cancellations caused by similarities between the signal and normalization modes. The uncertainty due to finite simulated sample sizes is evaluated using a bootstrapping technique [38]. The impact of different detector occupancies in data and simulation is evaluated by recomputing the efficiencies using an additional correction accounting for the deviations. The efficiency ratios are recomputed varying the parameters used to

TABLE II. Branching fractions of (top) $D^0 \rightarrow \pi^+\pi^-e^+e^-$ and (bottom) $D^0 \rightarrow K^+K^-e^+e^-$ decays in different ranges of dielectron mass. Shown in comparison on the right are the branching fractions of $D^0 \rightarrow \pi^+\pi^-\mu^+\mu^-$ and $D^0 \rightarrow K^+K^-\mu^+\mu^-$ decays in the corresponding dimuon-mass ranges from Ref. [20]. The uncertainties are statistical, systematic and due to the limited knowledge of the normalization branching fraction. The reported upper limits correspond to 90% (95%) confidence level. The correlations between the various dielectron-mass ranges are reported in the Supplemental Material [35].

$m(\ell^+\ell^-)$ region	[MeV/ c^2]	\mathcal{B} [10^{-7}]	
		$D^0 \rightarrow \pi^+\pi^-e^+e^-$	$D^0 \rightarrow \pi^+\pi^-\mu^+\mu^-$ [20]
Low mass	$2m_\mu$ –525	$<4.8(5.4)$	$0.78 \pm 0.19 \pm 0.05 \pm 0.08$
η	525–565	$<2.3(2.7)$	$<0.24(0.28)$
ρ^0/ω	565–950	$4.5 \pm 1.0 \pm 0.7 \pm 0.6$	$4.06 \pm 0.33 \pm 0.21 \pm 0.41$
ϕ	950–1100	$3.8 \pm 0.7 \pm 0.4 \pm 0.5$	$4.54 \pm 0.29 \pm 0.25 \pm 0.45$
High mass	>1100	$<2.0(2.2)$	$<0.28(0.33)$
		$D^0 \rightarrow K^+K^-e^+e^-$	$D^0 \rightarrow K^+K^-\mu^+\mu^-$ [20]
Low mass	$2m_\mu$ –525	$<1.0(1.1)$	$0.26 \pm 0.12 \pm 0.02 \pm 0.03$
η	525–565	$<0.4(0.5)$	$<0.07(0.08)$
ρ^0/ω	>565	$<2.2(2.5)$	$1.20 \pm 0.23 \pm 0.07 \pm 0.12$

smear the dielectron mass within their statistical uncertainties, and varying the resonant models of the signal decays within their uncertainties. In addition, the efficiency ratios are recomputed after artificially injecting an additional nonresonant component, representing unknown short-distance physics, into the simulated signal distributions at 10% of the total number of events. Relative variations of the efficiency ratio between approximately 7% and 14% are found in the dielectron-mass regions and taken as systematic uncertainties. The impact of charm hadrons produced in beauty hadron decays is evaluated and found to be negligible.

To summarize, the biggest systematic uncertainties arise from finite simulated sample sizes, the limited knowledge of the signal-decay resonant structure, and the models used in the fit. The total systematic uncertainty depends on the decay mode and dielectron-mass region and ranges between approximately 10% and 70% of the corresponding statistical precision [35].

Measured branching fractions for $D^0 \rightarrow \pi^+\pi^-e^+e^-$ and $D^0 \rightarrow K^+K^-e^+e^-$ decays in regions of $m(e^+e^-)$ are reported in Table II if the statistical significance exceeds 3 standard deviations, where the first uncertainty accounts for the statistical component, the second for the systematic, and the third corresponds to a 13.7% relative uncertainty on $\mathcal{B}(D^0 \rightarrow K^-\pi^+[e^+e^-]_{\rho^0/\omega})$ [25]. The Feldman-Cousins approach [39] is used to report the statistical uncertainties on the branching fractions. Upper limits are derived in all other $m(e^+e^-)$ regions using the CL_s method including the effects due to the systematic uncertainties [40,41]. For comparison, the known branching fractions of $D^0 \rightarrow \pi^+\pi^-\mu^+\mu^-$ and $D^0 \rightarrow K^+K^-\mu^+\mu^-$ decays, taken from Ref. [20], are also shown. Integrating over the dielectron-mass regions defined in Table II, and accounting for correlations [35], the total branching fraction for $D^0 \rightarrow \pi^+\pi^-e^+e^-$ decays with $m(e^+e^-)$ greater than 2

times the muon mass is measured to be

$$\begin{aligned} \mathcal{B}(D^0 \rightarrow \pi^+\pi^-[e^+e^-]_{m(e^+e^-)>2m_\mu}) \\ = (13.3 \pm 1.7 \pm 1.7 \pm 1.8) \times 10^{-7}, \end{aligned}$$

where the uncertainties are statistical, systematic and due to the limited knowledge of the normalization-mode branching fraction, respectively. The result is consistent with the SM expectations [5,6] and with the branching fraction of $D^0 \rightarrow \pi^+\pi^-\mu^+\mu^-$ of $(9.6 \pm 1.2) \times 10^{-7}$ [20]. No total branching fraction is quoted for $D^0 \rightarrow K^+K^-e^+e^-$ decays as no significant signal is observed in any of the dielectron-mass regions.

In summary, a study of the $D^0 \rightarrow \pi^+\pi^-e^+e^-$ and $D^0 \rightarrow K^+K^-e^+e^-$ decays is performed in regions of the dielectron mass using $p p$ collisions collected by the LHCb experiment at $\sqrt{s} = 13$ TeV. The decay $D^0 \rightarrow \pi^+\pi^-e^+e^-$ is observed for the first time when requiring that the two electrons are consistent with coming from the decay of a ϕ or ρ^0/ω mesons. No evidence is found for the $D^0 \rightarrow K^+K^-e^+e^-$ decay and world-best limits are set on its branching fraction which improves previous best limits by 2 orders of magnitude. The results are compared to, and found to be consistent with, the branching fractions of the $D^0 \rightarrow \pi^+\pi^-\mu^+\mu^-$ and $D^0 \rightarrow K^+K^-\mu^+\mu^-$ decays recently measured by LHCb, and confirm lepton universality at the current precision.

We express our gratitude to our colleagues in the CERN accelerator departments for the excellent performance of the LHC. We thank the technical and administrative staff at the LHCb institutes. We acknowledge support from CERN and from the national agencies: ARC (Australia); CAPES, CNPq, FAPERJ and FINEP (Brazil); MOST and NSFC (China); CNRS/IN2P3 (France); BMBF, DFG and MPG

(Germany); INFN (Italy); NWO (Netherlands); MNiSW and NCN (Poland); MCID/IFA (Romania); MICIU and AEI (Spain); SNSF and SER (Switzerland); NASU (Ukraine); STFC (United Kingdom); DOE NP and NSF (USA). We acknowledge the computing resources that are provided by ARDC (Australia), CBPF (Brazil), CERN, IHEP and LZU (China), IN2P3 (France), KIT and DESY (Germany), INFN (Italy), SURF (Netherlands), Polish WLCG (Poland), IFIN-HH (Romania), PIC (Spain), CSCS (Switzerland), and GridPP (United Kingdom). We are indebted to the communities behind the multiple open-source software packages on which we depend. Individual groups or members have received support from Key Research Program of Frontier Sciences of CAS, CAS PIFI, CAS CCEPP, Fundamental Research Funds for the

Central Universities, and Sci. & Tech. Program of Guangzhou (China); Minciencias (Colombia); EPLANET, Marie Skłodowska-Curie Actions, ERC and NextGenerationEU (European Union); A*MIDEX, ANR, IPhU and Labex P2IO, and Région Auvergne-Rhône-Alpes (France); Alexander-von-Humboldt Foundation (Germany); ICSC (Italy); Severo Ochoa and María de Maeztu Units of Excellence, GVA, XuntaGal, GENCAT, InTalent-Inditex and Prog. Atracción Talento CM (Spain); SRC (Sweden); the Leverhulme Trust, the Royal Society and UKRI (United Kingdom).

Data availability. The data supporting this study's findings are available within the article.

-
- [1] S. L. Glashow, J. Iliopoulos, and L. Maiani, Weak interactions with lepton-hadron symmetry, *Phys. Rev. D* **2**, 1285 (1970).
- [2] R. K. Ellis *et al.*, Physics briefing book: Input for the European strategy for particle physics update 2020, [arXiv:1910.11775](https://arxiv.org/abs/1910.11775).
- [3] A. Paul, I. I. Bigi, and S. Recksiegel, On $D \rightarrow X_u \ell^+ \ell^-$ within the standard model and frameworks like the littlest Higgs model with T parity, *Phys. Rev. D* **83**, 114006 (2011).
- [4] S. Fajfer, N. Košnik, and S. Prelovšek, Updated constraints on new physics in rare charm decays, *Phys. Rev. D* **76**, 074010 (2007).
- [5] L. Cappiello, O. Catà, and G. D'Ambrosio, Standard model prediction and new physics tests for $D^0 \rightarrow h_1^+ h_2^- \ell^+ \ell^-$ ($h = \pi, K; \ell = e, \mu$), *J. High Energy Phys.* **04** (2013) 135.
- [6] S. De Boer and G. Hiller, Null tests from angular distributions in $D \rightarrow P_1 P_2 \ell^+ \ell^-$, $\ell = e, \mu$ decays on and off peak, *Phys. Rev. D* **98**, 035041 (2018).
- [7] S. Fajfer and S. Prelovšek, Effects of littlest Higgs model in rare D meson decays, *Phys. Rev. D* **73**, 054026 (2006).
- [8] I. I. Bigi and A. Paul, On CP asymmetries in two-, three- and four-body D decays, *J. High Energy Phys.* **03** (2012) 021.
- [9] A. Paul, A. de la Puente, and I. I. Bigi, Manifestations of warped extra dimension in rare charm decays and asymmetries, *Phys. Rev. D* **90**, 014035 (2014).
- [10] S. Fajfer and N. Košnik, Resonance catalyzed CP asymmetries in $D \rightarrow P \ell^+ \ell^-$, *Phys. Rev. D* **87**, 054026 (2013).
- [11] S. Fajfer and N. Košnik, Prospects of discovering new physics in rare charm decays, *Eur. Phys. J. C* **75**, 567 (2015).
- [12] S. de Boer and G. Hiller, Flavour and new physics opportunities with rare charm decays into leptons, *Phys. Rev. D* **93**, 074001 (2016).
- [13] H. Gisbert, M. Golz, and D. S. Mitzel, Theoretical and experimental status of rare charm decays, *Mod. Phys. Lett. A* **36**, 2130002 (2021).
- [14] R. Bause, M. Golz, G. Hiller, and A. Tayduganov, The new physics reach of null tests with $D \rightarrow \pi \ell \ell$ and $D_s \rightarrow K \ell \ell$ decays, *Eur. Phys. J. C* **80**, 65 (2020); **81**, 219(E) (2021).
- [15] R. Bause, H. Gisbert, M. Golz, and G. Hiller, Exploiting CP -asymmetries in rare charm decays, *Phys. Rev. D* **101**, 115006 (2020).
- [16] A. Bharucha, D. Boito, and C. Méaux, Disentangling QCD and new physics in $D^+ \rightarrow \pi^+ \ell^+ \ell^-$, *J. High Energy Phys.* **04** (2021) 158.
- [17] S. Fajfer, E. Solomonidi, and L. Vale Silva, S -wave contribution to rare $D^0 \rightarrow \pi^+ \pi^- \ell^+ \ell^-$ decays in the standard model and sensitivity to new physics, *Phys. Rev. D* **109**, 036027 (2024).
- [18] M. Mandal, S. Biswas, S. Mahata, and S. Sahoo, Searching for new physics in $c \rightarrow \mu$ transitions with nonuniversal Z' model, *Int. J. Mod. Phys. A* **39**, 2450063 (2024).
- [19] H. Gisbert, G. Hiller, and D. Suelmann, Effective field theory analysis of rare $|\Delta c| = |\Delta u| = 1$ charm decays, *J. High Energy Phys.* **12** (2024) 102.
- [20] R. Aaij *et al.* (LHCb Collaboration), Observation of D^0 meson decays to $\pi^+ \pi^- \mu^+ \mu^-$ and $K^+ K^- \mu^+ \mu^-$ final states, *Phys. Rev. Lett.* **119**, 181805 (2017).
- [21] R. Aaij *et al.* (LHCb Collaboration), Measurement of angular and CP asymmetries in $D^0 \rightarrow \pi^+ \pi^- \mu^+ \mu^-$ and $D^0 \rightarrow K^+ K^- \mu^+ \mu^-$ decays, *Phys. Rev. Lett.* **121**, 091801 (2018).
- [22] R. Aaij *et al.* (LHCb Collaboration), Angular analysis of $D^0 \rightarrow \pi^+ \pi^- \mu^+ \mu^-$ and $D^0 \rightarrow K^+ K^- \mu^+ \mu^-$ decays and search for CP violation, *Phys. Rev. Lett.* **128**, 221801 (2022).
- [23] E. M. Aitala *et al.* (E791 Collaboration), Search for rare and forbidden charm meson decays $D^0 \rightarrow V \ell^+ \ell^-$ and $h h \ell \ell$, *Phys. Rev. Lett.* **86**, 3969 (2001).
- [24] M. Ablikim *et al.* (BESIII Collaboration), Search for the rare decays $D \rightarrow h(h') e^+ e^-$, *Phys. Rev. D* **97**, 072015 (2018).

- [25] J. P. Lees *et al.* (BABAR Collaboration), Observation of the decay $D^0 \rightarrow K^- \pi^+ e^+ e^-$, *Phys. Rev. Lett.* **122**, 081802 (2019).
- [26] A. A. Alves Jr. *et al.* (LHCb Collaboration), The LHCb detector at the LHC, *J. Instrum.* **3**, S08005 (2008).
- [27] R. Aaij *et al.* (LHCb Collaboration), LHCb detector performance, *Int. J. Mod. Phys. A* **30**, 1530022 (2015).
- [28] R. Aaij *et al.*, The LHCb trigger and its performance in 2011, *J. Instrum.* **8**, P04022 (2013).
- [29] L. Breiman, J. H. Friedman, R. A. Olshen, and C. J. Stone, *Classification and Regression Trees* (Wadsworth International Group, Belmont, California, 1984).
- [30] B. P. Roe, H.-J. Yang, J. Zhu, Y. Liu, I. Stancu, and G. McGregor, Boosted decision trees as an alternative to artificial neural networks for particle identification, *Nucl. Instrum. Methods Phys. Res., Sect. A* **543**, 577 (2005).
- [31] M. Clemencic, G. Corti, S. Easo, C. R. Jones, S. Miglioranza, M. Pappagallo, and P. Robbe, The LHCb simulation application, Gauss: Design, evolution and experience, *J. Phys. Conf. Ser.* **331**, 032023 (2011).
- [32] I. Belyaev *et al.*, Handling of the generation of primary events in Gauss, the LHCb simulation framework, *J. Phys. Conf. Ser.* **331**, 032047 (2011).
- [33] G. Punzi, Sensitivity of searches for new signals and its optimization, eConf C **030908**, MODT002 (2003).
- [34] S. Navas *et al.* (Particle Data Group), Review of particle physics, *Phys. Rev. D* **110**, 030001 (2024).
- [35] See Supplemental Material at <http://link.aps.org/supplemental/10.1103/PhysRevD.111.L091101> for the fit results of $D^0 \rightarrow K^- \pi^+ [e^+ e^-]_{\rho^0/\omega}$ and the measured branching fractions for $D^0 \rightarrow \pi^+ \pi^- e^+ e^-$ and $D^0 \rightarrow K^+ K^- e^+ e^-$ decays in all dielectron-mass regions with their systematic uncertainties and correlations.
- [36] T. Skwarnicki, A study of the radiative cascade transitions between the Upsilon-prime and Upsilon resonances, Ph.D. thesis, Institute of Nuclear Physics, Krakow, 1986 [Report No. DESY-F31-86-02], <http://inspirehep.net/record/230779/>.
- [37] A. D. Bukin, Fitting function for asymmetric peaks, [arXiv:0711.4449](https://arxiv.org/abs/0711.4449).
- [38] B. Efron, Bootstrap methods: Another look at the jackknife, *Ann. Stat.* **7**, 1 (1979).
- [39] G. J. Feldman and R. D. Cousins, Unified approach to the classical statistical analysis of small signals, *Phys. Rev. D* **57**, 3873 (1998).
- [40] A. L. Read, Presentation of search results: The CL_s technique, *J. Phys. G* **28**, 2693 (2002).
- [41] T. Junk, Confidence level computation for combining searches with small statistics, *Nucl. Instrum. Methods Phys. Res., Sect. A* **434**, 435 (1999).
- [42] See CERN Document Server at <https://cds.cern.ch/record/2919753/> for data associated to the plots in this publication as well as in the supplementary material.

R. Aaij¹⁶,³⁸ A. S. W. Abdelmotteleb⁵⁷ C. Abellan Beteta,⁵¹ F. Abudinén⁵⁷ T. Ackernley⁶¹ A. A. Adefisoye⁶⁹ B. Adeva⁴⁷ M. Adinolfi⁵⁵ P. Adlarson⁸² C. Agapopoulou¹⁴ C. A. Aidala,⁸³ Z. Ajaltouni,¹¹ S. Akar¹¹ K. Akiba³⁸ P. Albicocco²⁸ J. Albrecht^{19,b} F. Alessio⁴⁹ M. Alexander⁶⁰ Z. Aliouche⁶³ P. Alvarez Cartelle⁵⁶ R. Amalric¹⁶ S. Amato³ J. L. Amey⁵⁵ Y. Amhis¹⁴ L. An⁶ L. Anderlini²⁷ M. Andersson⁵¹ A. Andreianov⁴⁴ P. Andreola⁵¹ M. Andreotti²⁶ D. Andreou⁶⁹ A. Anelli^{31,49,c} D. Ao⁷ F. Archilli^{37,d} M. Argenton²⁶ S. Arguedas Cuendis^{9,49} A. Artamonov⁴⁴ M. Artuso⁶⁹ E. Aslanides¹³ R. Ataíde Da Silva⁵⁰ M. Atzeni⁶⁵ B. Audurier¹² D. Bacher⁶⁴ I. Bachiller Perea¹⁰ S. Bachmann²² M. Bachmayer⁵⁰ J. J. Back⁵⁷ P. Baladron Rodriguez⁴⁷ V. Balagura¹⁵ A. Balboni²⁶ W. Baldini²⁶ L. Balzani¹⁹ H. Bao⁷ J. Baptista de Souza Leite⁶¹ C. Barbero Pretel^{47,12} M. Barbeti²⁷ I. R. Barbosa⁷⁰ R. J. Barlow⁶³ M. Barnyakov²⁵ S. Barsuk¹⁴ W. Barter⁵⁹ J. Bartz⁶⁹ J. M. Basels¹⁷ S. Bashir⁴⁰ G. Bassi^{35,e} B. Batsukh⁵ P. B. Battista,¹⁴ A. Bay⁵⁰ A. Beck⁶⁵ M. Becker¹⁹ F. Bedeschi³⁵ I. B. Bediaga² N. A. Behling¹⁹ S. Belin⁴⁷ K. Belous⁴⁴ I. Belov²⁹ I. Belyaev³⁶ G. Benane¹³ G. Bencivenni²⁸ E. Ben-Haim¹⁶ A. Berezhnoy⁴⁴ R. Bernet⁵¹ S. Bernet Andres⁴⁵ A. Bertolin³³ C. Betancourt⁵¹ F. Betti⁵⁹ J. Bex⁵⁶ Ia. Bezshyiko⁵¹ J. Bhom⁴¹ M. S. Bieker¹⁹ N. V. Biesuz²⁶ P. Billoir¹⁶ A. Biolchini³⁸ M. Birch⁶² F. C. R. Bishop¹⁰ A. Bitadze⁶³ A. Bizzeti⁵⁷ T. Blake⁵⁷ F. Blanc⁵⁰ J. E. Blank¹⁹ S. Blusk⁶⁹ V. Bocharnikov⁴⁴ J. A. Boelhaeve¹⁹ O. Boente Garcia¹⁵ T. Boettcher⁶⁶ A. Bohare⁵⁹ A. Boldyrev⁴⁴ C. S. Bolognani⁷⁹ R. Bolzonella^{26,f} R. B. Bonacci¹ N. Bondar⁴⁴ A. Bordelius⁴⁹ F. Borgato^{33,g} S. Borghi⁶³ M. Borsato^{31,c} J. T. Borsuk⁴¹ E. Botalico⁶¹ S. A. Bouchiba⁵⁰ M. Bovill⁶⁴ T. J. V. Bowcock⁶¹ A. Boyer⁴⁹ C. Bozzi²⁶ J. D. Brandenburg⁸⁴ A. Brea Rodriguez⁵⁰ N. Breer¹⁹ J. Brodzicka⁴¹ A. Brossa Gonzalo^{47,a} J. Brown⁶¹ D. Brundu³² E. Buchanan⁵⁹ L. Buonincontri^{33,g} M. Burgos Marcos⁷⁹ A. T. Burke⁶³ C. Burr⁴⁹ J. S. Butter⁵⁶ J. Buytaert⁴⁹ W. Byczynski⁴⁹ S. Cadeddu³² H. Cai⁷⁴ A. C. Caillet¹⁶ R. Calabrese^{26,f} S. Calderon Ramirez⁹ L. Calefice⁴⁶ S. Cali²⁸ M. Calvi^{31,c} M. Calvo Gomez⁴⁵ P. Camargo Magalhaes^{2,h} J. I. Cambon Bouzas⁴⁷ P. Campana²⁸ D. H. Campora Perez⁷⁹ A. F. Campoverde Quezada⁷ S. Capelli³¹ L. Capriotti²⁶ R. Caravaca-Mora⁹ A. Carbone^{25,i} L. Carcedo Salgado⁴⁷ R. Cardinale^{29,j} A. Cardini³² P. Carniti^{31,c}

- L. Carus,²² A. Casais Vidal,⁶⁵ R. Caspary,²² G. Casse,⁶¹ M. Cattaneo,⁴⁹ G. Cavallero,^{26,49} V. Cavallini,^{26,f} S. Celani,²² S. Cesare,^{30,k} A. J. Chadwick,⁶¹ I. Chahrour,⁸³ M. Charles,¹⁶ Ph. Charpentier,⁴⁹
- E. Chatzianagnostou,³⁸ M. Chefdeville,¹⁰ C. Chen,¹³ S. Chen,⁵ Z. Chen,⁷ A. Chernov,⁴¹ S. Chernyshenko,⁵³ X. Chiotopoulos,⁷⁹ V. Chobanova,⁸¹ M. Chrzasczcz,⁴¹ A. Chubykin,⁴⁴ V. Chulikov,^{28,36} P. Ciambrone,²⁸ X. Cid Vidal,⁴⁷ G. Ciezarek,⁴⁹ P. Cifra,⁴⁹ P. E. L. Clarke,⁵⁹ M. Clemencic,⁴⁹ H. V. Cliff,⁵⁶ J. Closier,⁴⁹ C. Cocha Toapaxi,²² V. Coco,⁴⁹ J. Cogan,¹³ E. Cogneras,¹¹ L. Cojocariu,⁴³ S. Collaviti,⁵⁰ P. Collins,⁴⁹
- T. Colombo,⁴⁹ M. Colonna,¹⁹ A. Comerma-Montells,⁴⁶ L. Congedo,²⁴ A. Contu,³² N. Cooke,⁶⁰ I. Corredoira,⁴⁷ A. Correia,¹⁶ G. Corti,⁴⁹ J. J. Cottee Meldrum,⁵⁵ B. Couturier,⁴⁹ D. C. Craik,⁵¹ M. Cruz Torres,^{2,1} E. Curras Rivera,⁵⁰ R. Currie,⁵⁹ C. L. Da Silva,⁶⁸ S. Dadabaev,⁴⁴ L. Dai,⁷¹ X. Dai,⁴ E. Dall’Occo,⁴⁹ J. Dalseno,⁴⁷ C. D’Ambrosio,⁴⁹ J. Daniel,¹¹ A. Danilina,⁴⁴ P. d’Argent,²⁴ G. Darze,³ A. Davidson,⁵⁷ J. E. Davies,⁶³ O. De Aguiar Francisco,⁶³ C. De Angelis,^{32,m} F. De Benedetti,⁴⁹ J. de Boer,³⁸ K. De Bruyn,⁷⁸ S. De Capua,⁶³ M. De Cian,²² U. De Freitas Carneiro Da Graca,^{2,n} E. De Lucia,²⁸ J. M. De Miranda,² L. De Paula,³ M. De Serio,^{24,o} P. De Simone,²⁸ F. De Vellis,¹⁹ J. A. de Vries,⁷⁹ F. Debernardis,²⁴ D. Decamp,¹⁰ V. Dedu,¹³ S. Dekkers,¹ L. Del Buono,¹⁶ B. Delaney,⁶⁵ H.-P. Dembinski,¹⁹ J. Deng,⁸ V. Denysenko,⁵¹ O. Deschamps,¹¹ F. Dettori,^{32,m} B. Dey,⁷⁷ P. Di Nezza,²⁸ I. Diachkov,⁴⁴ S. Didenko,⁴⁴ S. Ding,⁶⁹ L. Dittmann,²² V. Dobishuk,⁵³ A. D. Docheva,⁶⁰ C. Dong,^{4,p} A. M. Donohoe,²³ F. Dordei,³² A. C. dos Reis,² A. D. Dowling,⁶⁹ W. Duan,⁷² P. Duda,⁸⁰ M. W. Dudek,⁴¹ L. Dufour,⁴⁹ V. Duk,³⁴ P. Durante,⁴⁹ M. M. Duras,⁸⁰ J. M. Durham,⁶⁸ O. D. Durmus,⁷⁷ A. Dziurda,⁴¹ A. Dzyuba,⁴⁴ S. Easo,⁵⁸ E. Eckstein,¹⁸ U. Egede,¹ A. Egorychev,⁴⁴ V. Egorychev,⁴⁴ S. Eisenhardt,⁵⁹ E. Ejopu,⁶³ L. Eklund,⁸² M. Elashri,⁶⁶ J. Ellbracht,¹⁹ S. Ely,⁶² A. Ene,⁴³ J. Eschle,⁶⁹ S. Esen,²² T. Evans,⁶³ F. Fabiano,³² L. N. Falcao,² Y. Fan,⁷ B. Fang,⁷ L. Fantini,^{34,49,q} M. Faria,⁵⁰ K. Farmer,⁵⁹ D. Fazzini,^{31,c} L. Felkowski,⁸⁰ M. Feng,^{5,7} M. Feo,² A. Fernandez Casani,⁴⁸ M. Fernandez Gomez,⁴⁷ A. D. Ferez,⁶⁷ F. Ferrari,²⁵ F. Ferreira Rodrigues,³ M. Ferrillo,⁵¹ M. Ferro-Luzzi,⁴⁹ S. Filippov,⁴⁴ R. A. Fini,²⁴ M. Fiorini,^{26,f} M. Firlej,⁴⁰ K. L. Fischer,⁶⁴ D. S. Fitzgerald,⁸³ C. Fitzpatrick,⁶³ T. Fiutowski,⁴⁰ F. Fleuret,¹⁵ M. Fontana,²⁵ L. F. Foreman,⁶³ R. Forty,⁴⁹ D. Foulds-Holt,⁵⁶ V. Franco Lima,³ M. Franco Sevilla,⁶⁷ M. Frank,⁴⁹ E. Franzoso,^{26,f} G. Frau,⁶³ C. Frei,⁴⁹ D. A. Friday,⁶³ J. Fu,⁷ Q. Führung,^{19,56,b} Y. Fujii,¹ T. Fulghesu,¹⁶ E. Gabriel,³⁸ G. Galati,²⁴ M. D. Galati,³⁸ A. Gallas Torreira,⁴⁷ D. Galli,^{25,i} S. Gambetta,⁵⁹ M. Gandelman,³ P. Gandini,³⁰ B. Ganie,⁶³ H. Gao,⁷ R. Gao,⁶⁴ T. Q. Gao,⁵⁶ Y. Gao,⁸ Y. Gao,⁶ Y. Gao,⁸ L. M. Garcia Martin,⁵⁰ P. Garcia Moreno,⁴⁶ J. García Pardiñas,⁴⁹ P. Gardner,⁶⁷ K. G. Garg,⁸ L. Garrido,⁴⁶ C. Gaspar,⁴⁹ L. L. Gerken,¹⁹ E. Gersabeck,⁶³ M. Gersabeck,²⁰ T. Gershon,⁵⁷ S. Ghizzo,^{29,j} Z. Ghorbanimoghaddam,⁵⁵ L. Giambastiani,^{33,g} F. I. Giasemis,^{16,r} V. Gibson,⁵⁶ H. K. Gienza,⁴² A. L. Gilman,⁶⁴ M. Giovannetti,²⁸ A. Gioventù,⁴⁶ L. Girardey,⁶³ C. Giugliano,^{26,f} M. A. Giza,⁴¹ E. L. Gkougkousis,⁶² F. C. Glaser,^{14,22} V. V. Gligorov,^{16,49} C. Göbel,⁷⁰ E. Golobardes,⁴⁵ D. Golubkov,⁴⁴ A. Golutvin,^{62,49,44} S. Gomez Fernandez,⁴⁶ W. Gomulka,⁴⁰ F. Goncalves Abrantes,⁶⁴ M. Goncerz,⁴¹ G. Gong,^{4,p} J. A. Gooding,¹⁹ I. V. Gorelov,⁴⁴ C. Gotti,³¹ E. Govorkova,⁶⁵ J. P. Grabowski,¹⁸ L. A. Granado Cardoso,⁴⁹ E. Graugés,⁴⁶ E. Graverini,^{50,s} L. Grazette,⁵⁷ G. Graziani,⁴³ A. T. Grecu,⁴³ L. M. Greeven,³⁸ N. A. Grieser,⁶⁶ L. Grillo,⁶⁰ S. Gromov,⁴⁴ C. Gu,¹⁵ M. Guarise,²⁶ L. Guerry,¹¹ V. Guliaeva,⁴⁴ P. A. Günther,²² A.-K. Guseinov,⁵⁰ E. Gushchin,⁴⁴ Y. Guz,^{6,49,44} T. Gys,⁴⁹ K. Habermann,¹⁸ T. Hadavizadeh,¹ C. Hadjivasiliou,⁶⁷ G. Haefeli,⁵⁰ C. Haen,⁴⁹ G. Hallett,⁵⁷ M. M. Halvorsen,⁴⁹ P. M. Hamilton,⁶⁷ J. Hammerich,⁶¹ Q. Han,³³ X. Han,^{22,49} S. Hansmann-Menzemer,²² L. Hao,⁷ N. Harnew,⁶⁴ T. H. Harris,¹ M. Hartmann,¹⁴ S. Hashmi,⁴⁰ J. He,^{7,t} F. Hemmer,⁴⁹ C. Henderson,⁶⁶ R. D. L. Henderson,^{1,57} A. M. Hennequin,⁴⁹ K. Hennessy,⁶¹ L. Henry,⁵⁰ J. Herd,⁶² P. Herrero Gascon,²² J. Heuel,¹⁷ A. Hicheur,³ G. Hijano Mendizabal,⁵¹ J. Horswill,⁶³ R. Hou,⁸ Y. Hou,¹¹ N. Howarth,⁶¹ J. Hu,⁷² W. Hu,⁶ X. Hu,^{4,p} W. Huang,⁷ W. Hulsbergen,³⁸ R. J. Hunter,⁵⁷ M. Hushchyn,⁴⁴ D. Hutchcroft,⁶¹ M. Idzik,⁴⁰ D. Ilin,⁴⁴ P. Ilten,⁶⁶ A. Inglessi,⁴⁴ A. Iniukhin,⁴⁴ A. Ishteev,⁴⁴ K. Ivshin,⁴⁴ R. Jacobsson,⁴⁹ H. Jage,¹⁷ S. J. Jaimes Elles,^{75,49,48} S. Jakobsen,⁴⁹ E. Jans,³⁸ B. K. Jashal,⁴⁸ A. Jawahery,⁶⁷ V. Jevtic,^{19,b} E. Jiang,⁶⁷ X. Jiang,^{5,7} Y. Jiang,⁷ Y. J. Jiang,⁶ M. John,⁶⁴ A. John Rubesh Rajan,²³ D. Johnson,⁵⁴ C. R. Jones,⁵⁶ T. P. Jones,⁵⁷ S. Joshi,⁴² B. Jost,⁴⁹ J. Juan Castella,⁵⁶ N. Jurik,⁴⁹ I. Juszcak,⁴¹ D. Kaminaris,⁵⁰ S. Kandybei,⁵² M. Kane,⁵⁹ Y. Kang,^{4,p} C. Kar,¹¹ M. Karacson,⁴⁹ D. Karpenkov,⁴⁴ A. Kauniskangas,⁵⁰ J. W. Kautz,⁶⁶ M. K. Kazanecki,⁴¹ F. Keizer,⁴⁹ M. Kenzie,⁵⁶ T. Ketel,³⁸ B. Khanji,⁶⁹ A. Kharisova,⁴⁴ S. Kholodenko,^{35,49} G. Khreich,¹⁴ T. Kirn,¹⁷ V. S. Kirsebom,³¹ O. Kitouni,⁶⁵ S. Klaver,³⁹

N. Kleijne^{35,e} K. Klimaszewski⁴² M.R. Kmiec⁴² S. Koliiev⁵³ L. Kolk¹⁹ A. Konoplyannikov⁴⁴
P. Kopciwicz⁴⁹ P. Koppenburg³⁸ M. Korolev⁴⁴ I. Kostiuk³⁸ O. Kot⁵³ S. Kotriakhova⁴⁴ A. Kozachuk⁴⁴
P. Kravchenko⁴⁴ L. Kravchuk⁴⁴ M. Kreps⁵⁷ P. Krokovny⁴⁴ W. Krupa⁶⁹ W. Krzemien⁴² O. Kshyvanskyi⁵³
S. Kubis⁸⁰ M. Kucharczyk⁴¹ V. Kudryavtsev⁴⁴ E. Kulikova⁴⁴ A. Kupsc⁸² B. K. Kutsenko¹³ D. Lacarrere⁴⁹
P. Laguarda Gonzalez⁴⁶ A. Lai³² A. Lampis³² D. Lancierini⁵⁶ C. Landesa Gomez⁴⁷ J. J. Lane¹ R. Lane⁵⁵
G. Lanfranchi²⁸ C. Langenbruch²² J. Langer¹⁹ O. Lantwin⁴⁴ T. Latham⁵⁷ F. Lazzari^{35,49,s} C. Lazzeroni⁵⁴
R. Le Gac¹³ H. Lee⁶¹ R. Lefèvre¹¹ A. Leflat⁴⁴ S. Legotin⁴⁴ M. Lehuraux⁵⁷ E. Lemos Cid⁴⁹ O. Leroy¹³
T. Lesiak⁴¹ E. D. Lesser⁴⁹ B. Leverington²² A. Li^{4,p} C. Li¹³ H. Li⁷² K. Li⁸ L. Li⁶³ M. Li⁸ P. Li⁷
P.-R. Li⁷³ Q. Li^{5,7} S. Li⁸ T. Li^{5,u} T. Li⁷² Y. Li⁸ Y. Li⁵ Z. Lian^{4,p} X. Liang⁶⁹ S. Libralon⁴⁸ C. Lin⁷
T. Lin⁵⁸ R. Lindner⁴⁹ H. Linton⁶² V. Lisovskyi⁵⁰ R. Litvinov^{32,49} F. L. Liu¹ G. Liu⁷² K. Liu⁷³ S. Liu^{5,7}
W. Liu⁸ Y. Liu⁵⁹ Y. Liu⁷³ Y. L. Liu⁶² G. Loachamin Ordonez⁷⁰ A. Lobo Salvia⁴⁶ A. Loi³² T. Long⁵⁶
J. H. Lopes³ A. Lopez Huertas⁴⁶ S. López Soliño⁴⁷ Q. Lu¹⁵ C. Lucarelli²⁷ D. Lucchesi^{33,g}
M. Lucio Martinez⁷⁹ V. Lukashenko^{38,53} Y. Luo⁶ A. Lupato^{33,v} E. Luppi^{26,f} K. Lynch²³ X.-R. Lyu⁷
G. M. Ma^{4,p} S. Maccolini¹⁹ F. Machefert¹⁴ F. Maciuc⁴³ B. Mack⁶⁹ I. Mackay⁶⁴ L. M. Mackey⁶⁹
L. R. Madhan Mohan⁵⁶ M. J. Madurai⁵⁴ A. Maevskiy⁴⁴ D. Magdalinski³⁸ D. Maisuzenko⁴⁴
J. J. Malczewski⁴¹ S. Malde⁶⁴ L. Malentacca⁴⁹ A. Malinin⁴⁴ T. Maltsev⁴⁴ G. Manca^{32,m} G. Mancinelli¹³
C. Mancuso³⁰ R. Manera Escalero⁴⁶ F. M. Manganella³⁷ D. Manuzzi²⁵ D. Marangotto^{30,k} J. F. Marchand¹⁰
R. Marchevski⁵⁰ U. Marconi²⁵ E. Mariani¹⁶ S. Mariani⁴⁹ C. Marin Benito⁴⁶ J. Marks²² A. M. Marshall⁵⁵
L. Martel⁶⁴ G. Martelli^{34,q} G. Martellotti³⁶ L. Martinazzoli⁴⁹ M. Martinelli^{31,c} D. Martinez Gomez⁷⁸
D. Martinez Santos⁸¹ F. Martinez Vidal⁴⁸ A. Martorell i Granollers⁴⁵ A. Massafferri² R. Matev⁴⁹ A. Mathad⁴⁹
V. Matiunin⁴⁴ C. Matteuzzi⁶⁹ K. R. Mattioli¹⁵ A. Mauri⁶² E. Maurice¹⁵ J. Mauricio⁴⁶ P. Mayencourt⁵⁰
J. Mazorra de Cos⁴⁸ M. Mazurek⁴² M. McCann⁶² T. H. McGrath⁶³ N. T. McHugh⁶⁰ A. McNab⁶³
R. McNulty²³ B. Meadows⁶⁶ G. Meier¹⁹ D. Melnychuk⁴² F. M. Meng^{4,p} M. Merk^{38,79} A. Merli⁵⁰
L. Meyer Garcia⁶⁷ D. Miao^{5,7} H. Miao⁷ M. Mikhasenko⁷⁶ D. A. Milanes^{75,w} A. Minotti^{31,c} E. Minucci²⁸
T. Miralles¹¹ B. Mitreska¹⁹ D. S. Mitzel¹⁹ A. Modak⁵⁸ L. Moeser¹⁹ R. A. Mohammed⁶⁴ R. D. Moise¹⁷
S. Mokhnenko⁴⁴ E. F. Molina Cardenas⁸³ T. Mombächer⁴⁹ M. Monk^{57,1} S. Monteil¹¹ A. Morcillo Gomez⁴⁷
G. Morello²⁸ M. J. Morello^{35,e} M. P. Morgenthaler²² J. Moron⁴⁰ W. Morren³⁸ A. B. Morris⁴⁹ A. G. Morris¹³
R. Mountain⁶⁹ H. Mu^{4,p} Z. M. Mu⁶ E. Muhammad⁵⁷ F. Muheim⁵⁹ M. Mulder⁷⁸ K. Müller⁵¹
F. Muñoz-Rojas⁹ R. Murta⁶² P. Naik⁶¹ T. Nakada⁵⁰ R. Nandakumar⁵⁸ T. Nanut⁴⁹ I. Nasteva³
M. Needham⁵⁹ N. Neri^{30,k} S. Neubert¹⁸ N. Neufeld⁴⁹ P. Neustroev⁴⁴ J. Nicolini¹⁹ D. Nicotra⁷⁹ E. M. Niel⁴⁹
N. Nikitin⁴⁴ Q. Niu⁷³ P. Nogarolli³ P. Nogga¹⁸ C. Normand⁵⁵ J. Novoa Fernandez⁴⁷ G. Nowak⁶⁶
C. Nunez⁸³ H. N. Nur⁶⁰ A. Oblakowska-Mucha⁴⁰ V. Obraztsov⁴⁴ T. Oeser¹⁷ S. Okamura^{26,f} A. Okhotnikov⁴⁴
O. Okhrimenko⁵³ R. Oldeman^{32,m} F. Oliva⁵⁹ M. Olocco¹⁹ C. J. G. Onderwater⁷⁹ R. H. O'Neil⁴⁹ D. Osthues¹⁹
J. M. Otalora Goicochea³ P. Owen⁵¹ A. Oyanguren⁴⁸ O. Ozcelik⁵⁹ F. Paciolla^{35,x} A. Padee⁴²
K. O. Padeken¹⁸ B. Pagare⁵⁷ P. R. Pais²² T. Pajero⁴⁹ A. Palano²⁴ M. Palutan²⁸ X. Pan^{4,p} G. Panshin⁴⁴
L. Paolucci⁵⁷ A. Papanestis^{58,49} M. Pappagallo^{24,o} L. L. Pappalardo^{26,f} C. Pappenheimer⁶⁶ C. Parkes⁶³
D. Parmar⁷⁶ B. Passalacqua^{26,f} G. Passaleva²⁷ D. Passaro^{35,49,e} A. Pastore²⁴ M. Patel⁶² J. Patoc⁶⁴
C. Patrignani^{25,i} A. Paul⁶⁹ C. J. Pawley⁷⁹ A. Pellegrino³⁸ J. Peng^{5,7} M. Pepe Altarelli²⁸ S. Perazzini²⁵
D. Pereima⁴⁴ H. Pereira Da Costa⁶⁸ A. Pereiro Castro⁴⁷ P. Perret¹¹ A. Perrevoort⁷⁸ A. Perro^{49,13} M. J. Peters⁶⁶
K. Petridis⁵⁵ A. Petrolini^{29,j} J. P. Pfaller⁶⁶ H. Pham⁶⁹ L. Pica^{35,e} M. Piccini³⁴ L. Piccolo³² B. Pietrzyk¹⁰
G. Pietrzyk¹⁴ R. N. Pilato⁶¹ D. Pinci³⁶ F. Pisani⁴⁹ M. Pizzichemi^{31,49,c} V. Placinta⁴³ M. Plo Casaus⁴⁷
T. Poeschl⁴⁹ F. Polci¹⁶ M. Poli Lener²⁸ A. Poluektov¹³ N. Polukhina⁴⁴ I. Polyakov⁴⁴ E. Polycarpo³
S. Ponce⁴⁹ D. Popov⁷ S. Poslavskii⁴⁴ K. Prasanth⁵⁹ C. Prouve⁸¹ D. Provenzano^{32,m} V. Pugatch⁵³
G. Punzi^{35,s} S. Qasim⁵¹ Q. Q. Qian⁶ W. Qian⁷ N. Qin^{4,p} S. Qu^{4,p} R. Quagliani⁴⁹ R. I. Rabadan Trejo⁵⁷
J. H. Rademacker⁵⁵ M. Rama³⁵ M. Ramírez García⁸³ V. Ramos De Oliveira⁷⁰ M. Ramos Pernas⁵⁷
M. S. Rangel³ F. Ratnikov⁴⁴ G. Raven³⁹ M. Rebollo De Miguel⁴⁸ F. Redi^{30,v} J. Reich⁵⁵ F. Reiss²⁰ Z. Ren⁷
P. K. Resmi⁶⁴ R. Ribatti⁵⁰ G. R. Ricart^{15,12} D. Riccardi^{35,e} S. Ricciardi⁵⁸ K. Richardson⁶⁵
M. Richardson-Slipper⁵⁹ K. Rinnert⁶¹ P. Robbe^{14,49} G. Robertson⁶⁰ E. Rodrigues⁶¹ A. Rodriguez Alvarez⁴⁶
E. Rodriguez Fernandez⁴⁷ J. A. Rodriguez Lopez⁷⁵ E. Rodriguez Rodriguez⁴⁹ J. Roensch¹⁹ A. Rogachev⁴⁴

A. Rogovskiy⁵⁸, D. L. Rolf⁴⁹, P. Roloff⁴⁹, V. Romanovskiy⁶⁶, A. Romero Vidal⁴⁷, G. Romolini²⁶, F. Ronchetti⁵⁰, T. Rong⁶, M. Rotondo²⁸, S. R. Roy²², M. S. Rudolph⁶⁹, M. Ruiz Diaz²², R. A. Ruiz Fernandez⁴⁷, J. Ruiz Vidal^{82,y}, A. Ryzhikov⁴⁴, J. Ryzka⁴⁰, J. J. Saavedra-Arias⁹, J. J. Saborido Silva⁴⁷, R. Sadek¹⁵, N. Sagidova⁴⁴, D. Sahoo⁷⁷, N. Sahoo⁵⁴, B. Saitta^{32,m}, M. Salomoni^{31,49,c}, I. Sanderswood⁴⁸, R. Santacesaria³⁶, C. Santamarina Rios⁴⁷, M. Santimaria²⁸, L. Santoro², E. Santovetti³⁷, A. Saputi^{26,49}, D. Saranin⁴⁴, A. Sarnatskiy⁷⁸, G. Sarpis⁵⁹, M. Sarpis⁶³, C. Satriano^{36,z}, A. Satta³⁷, M. Saur⁶, D. Savrina⁴⁴, H. Sazak¹⁷, F. Sborzacchi^{49,28}, L. G. Scantlebury Smead⁶⁴, A. Scarabotto¹⁹, S. Schael¹⁷, S. Scherl⁶¹, M. Schiller⁶⁰, H. Schindler⁴⁹, M. Schmelling²¹, B. Schmidt⁴⁹, S. Schmitt¹⁷, H. Schmitz¹⁸, O. Schneider⁵⁰, A. Schopper⁴⁹, N. Schulte¹⁹, S. Schulte⁵⁰, M. H. Schune¹⁴, R. Schwemmer⁴⁹, G. Schwering¹⁷, B. Sciascia²⁸, A. Sciuccati⁴⁹, I. Segal⁷⁶, S. Sellam⁴⁷, A. Semennikov⁴⁴, T. Senger⁵¹, M. Senghi Soares³⁹, A. Sergi^{29,j}, N. Serra⁵¹, L. Sestini³³, A. Seuthe¹⁹, Y. Shang⁶, D. M. Shangase⁸³, M. Shapkin⁴⁴, R. S. Sharma⁶⁹, I. Shchemerov⁴⁴, L. Shchutska⁵⁰, T. Shears⁶¹, L. Shekhtman⁴⁴, Z. Shen⁶, S. Sheng^{5,7}, V. Shevchenko⁴⁴, B. Shi⁷, Q. Shi⁷, Y. Shimizu¹⁴, E. Shmanin²⁵, R. Shorkin⁴⁴, J. D. Shupperd⁶⁹, R. Silva Coutinho⁶⁹, G. Simi^{33,g}, S. Simone^{24,o}, N. Skidmore⁵⁷, T. Skwarnicki⁶⁹, M. W. Slater⁵⁴, J. C. Smallwood⁶⁴, E. Smith⁶⁵, K. Smith⁶⁸, M. Smith⁶², A. Snoch³⁸, L. Soares Lavra⁵⁹, M. D. Sokoloff⁶⁶, F. J. P. Soler⁶⁰, A. Solomin^{44,55}, A. Solovev⁴⁴, I. Solovyev⁴⁴, N. S. Sommerfeld¹⁸, R. Song¹, Y. Song⁵⁰, Y. Song^{4,p}, Y. S. Song⁶, F. L. Souza De Almeida⁶⁹, B. Souza De Paula³, E. Spadaro Norella^{29,j}, E. Spedicato²⁵, J. G. Speer¹⁹, E. Spiridenkov⁴⁴, P. Spradlin⁶⁰, V. Sriskaran⁴⁹, F. Stagni⁴⁹, M. Stahl⁷⁶, S. Stahl⁴⁹, S. Stanislaus⁶⁴, M. Stefaniak⁸⁴, E. N. Stein⁴⁹, O. Steinkamp⁵¹, O. Stenyakin⁴⁴, H. Stevens¹⁹, D. Strelakina⁴⁴, Y. Su⁷, F. Suljik⁶⁴, J. Sun³², L. Sun⁷⁴, D. Sundfeld², W. Sutcliffe⁵¹, P. N. Swallow⁵⁴, K. Swientek⁴⁰, F. Swystun⁵⁶, A. Szabelski⁴², T. Szumlak⁴⁰, Y. Tan^{4,p}, Y. Tang⁷⁴, M. D. Tat²², A. Terentev⁴⁴, F. Terzuoli^{35,49,x}, F. Teubert⁴⁹, E. Thomas⁴⁹, D. J. D. Thompson⁵⁴, H. Tilquin⁶², V. Tisserand¹¹, S. T'Jampens¹⁰, M. Tobin^{5,49}, L. Tomassetti^{26,f}, G. Tonani^{30,k}, X. Tong⁶, T. Tork³⁰, D. Torres Machado², L. Toscano¹⁹, D. Y. Tou^{4,p}, C. Trippel⁴⁵, G. Tuci²², N. Tuning³⁸, L. H. Uecker²², A. Ukleja⁴⁰, D. J. Unverzagt²², B. Urbach⁵⁹, A. Usachov³⁹, A. Ustyuzhanin⁴⁴, U. Uwer²², V. Vagnoni²⁵, V. Valcarce Cadenas⁴⁷, G. Valenti²⁵, N. Valls Canudas⁴⁹, J. van Eldik⁴⁹, H. Van Hecke⁶⁸, E. van Herwijnen⁶², C. B. Van Hulse^{47,aa}, R. Van Laak⁵⁰, M. van Veghel³⁸, G. Vasquez⁵¹, R. Vazquez Gomez⁴⁶, P. Vazquez Regueiro⁴⁷, C. Vázquez Sierra⁴⁷, S. Vecchi²⁶, J. J. Velthuis⁵⁵, M. Veltri^{27,bb}, A. Venkateswaran⁵⁰, M. Verdoglia³², M. Vesterinen⁵⁷, D. Vico Benet⁶⁴, P. Vidrier Villalba⁴⁶, M. Vieites Diaz⁴⁷, X. Vilasis-Cardona⁴⁵, E. Vilella Figueras⁶¹, A. Villa²⁵, P. Vincent¹⁶, F. C. Volle⁵⁴, D. vom Bruch¹³, N. Voropaev⁴⁴, K. Vos⁷⁹, C. Vrahas⁵⁹, J. Wagner¹⁹, J. Walsh³⁵, E. J. Walton^{1,57}, G. Wan⁶, C. Wang²², G. Wang⁸, H. Wang⁷³, J. Wang⁶, J. Wang⁵, J. Wang^{4,p}, J. Wang⁷⁴, M. Wang⁴⁹, N. W. Wang⁷, R. Wang⁵⁵, X. Wang⁸, X. Wang⁷², X. W. Wang⁶², Y. Wang⁶, Y. W. Wang⁷³, Z. Wang¹⁴, Z. Wang^{4,p}, Z. Wang³⁰, J. A. Ward^{57,1}, M. Waterlaet⁴⁹, N. K. Watson⁵⁴, D. Websdale⁶², Y. Wei⁶, J. Wendel⁸¹, B. D. C. Westhenry⁵⁵, C. White⁵⁶, M. Whitehead⁶⁰, E. Whiter⁵⁴, A. R. Wiederhold⁶³, D. Wiedner¹⁹, G. Wilkinson⁶⁴, M. K. Wilkinson⁶⁶, M. Williams⁶⁵, M. J. Williams⁴⁹, M. R. J. Williams⁵⁹, R. Williams⁵⁶, Z. Williams⁵⁵, F. F. Wilson⁵⁸, M. Winn¹², W. Wislicki⁴², M. Witek⁴¹, L. Witola²², G. Wormser¹⁴, S. A. Wotton⁵⁶, H. Wu⁶⁹, J. Wu⁸, X. Wu⁷⁴, Y. Wu⁶, Z. Wu⁷, K. Wyllie⁴⁹, S. Xian⁷², Z. Xiang⁵, Y. Xie⁸, T. X. Xing³⁰, A. Xu³⁵, L. Xu^{4,p}, L. Xu^{4,p}, M. Xu⁵⁷, Z. Xu⁴⁹, Z. Xu⁷, Z. Xu⁵, K. Yang⁶², S. Yang⁷, X. Yang⁶, Y. Yang^{29,j}, Z. Yang⁶, V. Yeroshenko¹⁴, H. Yeung⁶³, H. Yin⁸, X. Yin⁷, C. Y. Yu⁶, J. Yu⁷¹, X. Yuan⁵, Y. Yuan^{5,7}, E. Zaffaroni⁵⁰, M. Zavertyaev²¹, M. Zdybal⁴¹, F. Zenesini²⁵, C. Zeng^{5,7}, M. Zeng^{4,p}, C. Zhang⁶, D. Zhang⁸, J. Zhang⁷, L. Zhang^{4,p}, S. Zhang⁷¹, S. Zhang⁶⁴, Y. Zhang⁶, Y. Z. Zhang^{4,p}, Z. Zhang^{4,p}, Y. Zhao²², A. Zhelezov²², S. Z. Zheng⁶, X. Z. Zheng^{4,p}, Y. Zheng⁷, T. Zhou⁶, X. Zhou⁸, Y. Zhou⁷, V. Zhovkovska⁵⁷, L. Z. Zhu⁷, X. Zhu^{4,p}, X. Zhu⁸, V. Zhukov¹⁷, J. Zhuo⁴⁸, Q. Zou^{5,7}, D. Zuliani^{33,g} and G. Zunica⁵⁰

(LHCb Collaboration)

¹*School of Physics and Astronomy, Monash University, Melbourne, Australia*²*Centro Brasileiro de Pesquisas Físicas (CBPF), Rio de Janeiro, Brazil*³*Universidade Federal do Rio de Janeiro (UFRJ), Rio de Janeiro, Brazil*⁴*Department of Engineering Physics, Tsinghua University, Beijing, China*

- ⁵*Institute of High Energy Physics (IHEP), Beijing, China*
- ⁶*School of Physics State Key Laboratory of Nuclear Physics and Technology, Peking University, Beijing, China*
- ⁷*University of Chinese Academy of Sciences, Beijing, China*
- ⁸*Institute of Particle Physics, Central China Normal University, Wuhan, Hubei, China*
- ⁹*Consejo Nacional de Rectores (CONARE), San Jose, Costa Rica*
- ¹⁰*Université Savoie Mont Blanc, CNRS, IN2P3-LAPP, Annecy, France*
- ¹¹*Université Clermont Auvergne, CNRS/IN2P3, LPC, Clermont-Ferrand, France*
- ¹²*Université Paris-Saclay, Centre d'Etudes de Saclay (CEA), IRFU, Saclay, France, Gif-Sur-Yvette, France*
- ¹³*Aix Marseille Univ, CNRS/IN2P3, CPPM, Marseille, France*
- ¹⁴*Université Paris-Saclay, CNRS/IN2P3, IJCLab, Orsay, France*
- ¹⁵*Laboratoire Leprince-Ringuet, CNRS/IN2P3, Ecole Polytechnique, Institut Polytechnique de Paris, Palaiseau, France*
- ¹⁶*LPNHE, Sorbonne Université, Paris Diderot Sorbonne Paris Cité, CNRS/IN2P3, Paris, France*
- ¹⁷*I. Physikalisches Institut, RWTH Aachen University, Aachen, Germany*
- ¹⁸*Universität Bonn—Helmholtz-Institut für Strahlen und Kernphysik, Bonn, Germany*
- ¹⁹*Fakultät Physik, Technische Universität Dortmund, Dortmund, Germany*
- ²⁰*Physikalisches Institut, Albert-Ludwigs-Universität Freiburg, Freiburg, Germany*
- ²¹*Max-Planck-Institut für Kernphysik (MPIK), Heidelberg, Germany*
- ²²*Physikalisches Institut, Ruprecht-Karls-Universität Heidelberg, Heidelberg, Germany*
- ²³*School of Physics, University College Dublin, Dublin, Ireland*
- ²⁴*INFN Sezione di Bari, Bari, Italy*
- ²⁵*INFN Sezione di Bologna, Bologna, Italy*
- ²⁶*INFN Sezione di Ferrara, Ferrara, Italy*
- ²⁷*INFN Sezione di Firenze, Firenze, Italy*
- ²⁸*INFN Laboratori Nazionali di Frascati, Frascati, Italy*
- ²⁹*INFN Sezione di Genova, Genova, Italy*
- ³⁰*INFN Sezione di Milano, Milano, Italy*
- ³¹*INFN Sezione di Milano-Bicocca, Milano, Italy*
- ³²*INFN Sezione di Cagliari, Monserrato, Italy*
- ³³*INFN Sezione di Padova, Padova, Italy*
- ³⁴*INFN Sezione di Perugia, Perugia, Italy*
- ³⁵*INFN Sezione di Pisa, Pisa, Italy*
- ³⁶*INFN Sezione di Roma La Sapienza, Roma, Italy*
- ³⁷*INFN Sezione di Roma Tor Vergata, Roma, Italy*
- ³⁸*Nikhef National Institute for Subatomic Physics, Amsterdam, Netherlands*
- ³⁹*Nikhef National Institute for Subatomic Physics and VU University Amsterdam, Amsterdam, Netherlands*
- ⁴⁰*AGH—University of Krakow, Faculty of Physics and Applied Computer Science, Kraków, Poland*
- ⁴¹*Henryk Niewodniczanski Institute of Nuclear Physics Polish Academy of Sciences, Kraków, Poland*
- ⁴²*National Center for Nuclear Research (NCBJ), Warsaw, Poland*
- ⁴³*Horia Hulubei National Institute of Physics and Nuclear Engineering, Bucharest-Magurele, Romania*
- ⁴⁴*Authors affiliated with an institute formerly covered by a cooperation agreement with CERN*
- ⁴⁵*DS4DS, La Salle, Universitat Ramon Llull, Barcelona, Spain*
- ⁴⁶*ICCUB, Universitat de Barcelona, Barcelona, Spain*
- ⁴⁷*Instituto Galego de Física de Altas Enerxías (IGFAE), Universidade de Santiago de Compostela, Santiago de Compostela, Spain*
- ⁴⁸*Instituto de Física Corpuscular, Centro Mixto Universidad de Valencia—CSIC, Valencia, Spain*
- ⁴⁹*European Organization for Nuclear Research (CERN), Geneva, Switzerland*
- ⁵⁰*Institute of Physics, Ecole Polytechnique Fédérale de Lausanne (EPFL), Lausanne, Switzerland*
- ⁵¹*Physik-Institut, Universität Zürich, Zürich, Switzerland*
- ⁵²*NSC Kharkiv Institute of Physics and Technology (NSC KIPT), Kharkiv, Ukraine*
- ⁵³*Institute for Nuclear Research of the National Academy of Sciences (KINR), Kyiv, Ukraine*
- ⁵⁴*School of Physics and Astronomy, University of Birmingham, Birmingham, United Kingdom*
- ⁵⁵*H.H. Wills Physics Laboratory, University of Bristol, Bristol, United Kingdom*
- ⁵⁶*Cavendish Laboratory, University of Cambridge, Cambridge, United Kingdom*
- ⁵⁷*Department of Physics, University of Warwick, Coventry, United Kingdom*
- ⁵⁸*STFC Rutherford Appleton Laboratory, Didcot, United Kingdom*
- ⁵⁹*School of Physics and Astronomy, University of Edinburgh, Edinburgh, United Kingdom*
- ⁶⁰*School of Physics and Astronomy, University of Glasgow, Glasgow, United Kingdom*

- ⁶¹*Oliver Lodge Laboratory, University of Liverpool, Liverpool, United Kingdom*
⁶²*Imperial College London, London, United Kingdom*
- ⁶³*Department of Physics and Astronomy, University of Manchester, Manchester, United Kingdom*
⁶⁴*Department of Physics, University of Oxford, Oxford, United Kingdom*
⁶⁵*Massachusetts Institute of Technology, Cambridge, Massachusetts, USA*
⁶⁶*University of Cincinnati, Cincinnati, Ohio, USA*
⁶⁷*University of Maryland, College Park, Maryland, USA*
- ⁶⁸*Los Alamos National Laboratory (LANL), Los Alamos, New Mexico, USA*
⁶⁹*Syracuse University, Syracuse, New York, USA*
- ⁷⁰*Pontifícia Universidade Católica do Rio de Janeiro (PUC-Rio), Rio de Janeiro, Brazil*
(associated with Universidade Federal do Rio de Janeiro (UFRJ), Rio de Janeiro, Brazil)
⁷¹*School of Physics and Electronics, Hunan University, Changsha City, China*
(associated with Institute of Particle Physics, Central China Normal University, Wuhan, Hubei, China)
- ⁷²*Guangdong Provincial Key Laboratory of Nuclear Science, Guangdong-Hong Kong Joint Laboratory of Quantum Matter, Institute of Quantum Matter, South China Normal University, Guangzhou, China*
(associated with Department of Engineering Physics, Tsinghua University, Beijing, China)
⁷³*Lanzhou University, Lanzhou, China*
(associated with Institute of High Energy Physics (IHEP), Beijing, China)
⁷⁴*School of Physics and Technology, Wuhan University, Wuhan, China*
(associated with Department of Engineering Physics, Tsinghua University, Beijing, China)
- ⁷⁵*Departamento de Física, Universidad Nacional de Colombia, Bogota, Colombia*
(associated with LPNHE, Sorbonne Université, Paris Diderot Sorbonne Paris Cité, CNRS/IN2P3, Paris, France)
- ⁷⁶*Ruhr Universitaet Bochum, Fakultät für Physik und Astronomie, Bochum, Germany*
(associated with Fakultät Physik, Technische Universität Dortmund, Dortmund, Germany)
⁷⁷*Eotvos Lorand University, Budapest, Hungary*
(associated with European Organization for Nuclear Research (CERN), Geneva, Switzerland)
- ⁷⁸*Van Swinderen Institute, University of Groningen, Groningen, Netherlands*
(associated with Nikhef National Institute for Subatomic Physics, Amsterdam, Netherlands)
⁷⁹*Universiteit Maastricht, Maastricht, Netherlands*
(associated with Nikhef National Institute for Subatomic Physics, Amsterdam, Netherlands)
- ⁸⁰*Tadeusz Kosciuszko Cracow University of Technology, Cracow, Poland*
(associated with Henryk Niewodniczanski Institute of Nuclear Physics Polish Academy of Sciences, Kraków, Poland)
⁸¹*Universidad da Coruña, A Coruña, Spain*
(associated with DS4DS, La Salle, Universitat Ramon Llull, Barcelona, Spain)
- ⁸²*Department of Physics and Astronomy, Uppsala University, Uppsala, Sweden*
(associated with School of Physics and Astronomy, University of Glasgow, Glasgow, United Kingdom)
- ⁸³*University of Michigan, Ann Arbor, Michigan, USA*
(associated with Syracuse University, Syracuse, New York, USA)
⁸⁴*The Ohio State University, Columbus, Ohio, USA*
(associated with Los Alamos National Laboratory (LANL), Los Alamos, New Mexico, USA)

^aDeceased.^bAlso at Lamarr Institute for Machine Learning and Artificial Intelligence, Dortmund, Germany.^cAlso at Università degli Studi di Milano-Bicocca, Milano, Italy.^dAlso at Università di Roma Tor Vergata, Roma, Italy.^eAlso at Scuola Normale Superiore, Pisa, Italy.^fAlso at Università di Ferrara, Ferrara, Italy.^gAlso at Università di Padova, Padova, Italy.^hAlso at Facultad de Ciencias Físicas, Madrid, Spain.ⁱAlso at Università di Bologna, Bologna, Italy.^jAlso at Università di Genova, Genova, Italy.^kAlso at Università degli Studi di Milano, Milano, Italy.^lAlso at Universidad Nacional Autónoma de Honduras, Tegucigalpa, Honduras.^mAlso at Università di Cagliari, Cagliari, Italy.

ⁿAlso at Centro Federal de Educação Tecnológica Celso Suckow da Fonseca, Rio De Janeiro, Brazil.

^oAlso at Università di Bari, Bari, Italy.

^pAlso at Center for High Energy Physics, Tsinghua University, Beijing, China.

^qAlso at Università di Perugia, Perugia, Italy.

^rAlso at LIP6, Sorbonne Université, Paris, France.

^sAlso at Università di Pisa, Pisa, Italy.

^tAlso at Hangzhou Institute for Advanced Study, UCAS, Hangzhou, China.

^uAlso at School of Physics and Electronics, Henan University, Kaifeng, China.

^vAlso at Università di Bergamo, Bergamo, Italy.

^wAlso at Universidad de Ingeniería y Tecnología (UTEC), Lima, Peru.

^xAlso at Università di Siena, Siena, Italy.

^yAlso at Department of Physics/Division of Particle Physics, Lund, Sweden.

^zAlso at Università della Basilicata, Potenza, Italy.

^{aa}Also at Universidad de Alcalá, Alcalá de Henares, Spain.

^{bb}Also at Università di Urbino, Urbino, Italy.